



# Experimental study on ultrasonic vibration–assisted drilling micro-hole of SiC<sub>f</sub>/SiC ceramic matrix composites

Bo Huang<sup>1,2</sup> · Wenhui Wang<sup>1,2</sup> · Ruisong Jiang<sup>3</sup> · Yifeng Xiong<sup>1,2</sup> · Cong Liu<sup>1,2</sup>

Received: 11 November 2021 / Accepted: 3 April 2022 / Published online: 6 May 2022  
© The Author(s), under exclusive licence to Springer-Verlag London Ltd., part of Springer Nature 2022

## Abstract

SiC<sub>f</sub>/SiC CMC has a broad range of applications, especially under extreme conditions, due to its excellent properties including high strength and stiffness, high wear and temperature resistance. However, these properties also bring new challenges to manufacturing. Traditional machining methods and ordinary cutting tools failed to fabricate high-quality parts that meet the manufacturing requirement, especially for drilling micro-holes. This paper intends to compare six commonly used tools for micro-hole drilling of SiC<sub>f</sub>/SiC CMC assisted by ultrasonic vibration: carbide drill, PCD drill, electroplated diamond abrasive tool, grinding drill, coated grinding drill, and PDC tool. First, the material removal process is theoretically analyzed, and the difference in tool life and machining quality of different cutting tools is analyzed from the point of view of the material removal process. Then, the influence of different kinds of tools on cutting forces, machining accuracy, and tool wear was also investigated through experiments, and the correctness of theoretical analysis was verified by experiments. The results show that the machining accuracy of the PDC tool is best, followed by the electroplated diamond abrasive tool. The machining accuracy of the grinding drill and coated grinding drill is poor with a bit of difference; PDC and coated grinding drill have less tool wear, while the grinding drill has slightly more severe tool wear. However, the tool wear of the electroplated diamond abrasive tool is severe. In summary, PDC tools are ideal for preparing SiC<sub>f</sub>/SiC composites.

**Keywords** SiC<sub>f</sub>/SiC · Ultrasonic vibration · Drilling · Micro-hole · Ceramic matrix composite

## 1 Introduction

Silicon carbide fiber reinforced silicon carbide ceramic matrix composites (SiC<sub>f</sub>/SiC CMC) have been attracting increasing attention due to their outstanding characteristics of high strength and stiffness, high temperature and wear resistance, low density, chemical stability, and so on [1–6].

Therefore, it is one of the ideal materials for hot-end components in aero-engines, especially hollow turbo-blades. The hollow turbo-blades have many micro-holes for cooling down. However, the high hardness, brittleness, and wear resistance of SiC<sub>f</sub>/SiC CMC bring new challenges to the hole drilling process. First, there is an increased risk of breaking the drilling tool considering the small hole diameter. Second, it is also challenging to carry out the drilling process due to the large drilling force and severe tool wear using traditional drilling methods. Therefore, it is vital to investigate micro-hole drilling of SiC<sub>f</sub>/SiC CMC.

At present, the commonly used micro-hole machining methods for ceramic matrix composites (CMC) are as follows: mechanical machining, electrical discharge machining (EDM), high-pressure water jet machining, electronic beam machining, laser machining, etc. Many previous studies have shown that tool wear is severe when carbide fiber reinforced silicon carbide ceramic matrix composites (C<sub>f</sub>/SiC CMC) are machined with traditional drilling methods. Meanwhile, fiber pull-out and edge break damage are easily caused during machining. Jiao et al. [7] machined SiC<sub>f</sub>/SiC CMC by

✉ Yifeng Xiong  
xiongyf@nwpu.edu.cn

<sup>1</sup> Key Laboratory of High Performance Manufacturing for Aero Engine, Ministry of Industry and Information Technology, School of Mechanical Engineering, Northwestern Polytechnical University, Xi'an, Shaanxi 710072, People's Republic of China

<sup>2</sup> Engineering Research Center of Advanced Manufacturing Technology for Aero Engine, Ministry of Education, School of Mechanical Engineering, Northwestern Polytechnical University, Xi'an, Shaanxi 710072, People's Republic of China

<sup>3</sup> School of Aeronautics and Astronautics, Sichuan University, Chengdu, Sichuan 610065, People's Republic of China

high-pressure water jet machining. The results showed that the exposed fiber section is more uneven, and the cut part of the fiber bundle appears to be pulled out. Therefore, high-pressure water jet machining is more suitable for the rough machining of SiC<sub>f</sub>/SiC CMC. Kliuev [8] added assisting electrode to machine SiC<sub>f</sub>/SiC CMC based on EDM. The results showed that it is easy to form remelting layer on the hole wall of SiC<sub>f</sub>/SiC CMC by EDM, and the electrode loss is more severe than that of ordinary EDM, and the machining efficiency is also significantly reduced. Wang et al. [9] conducted femtosecond laser experiments to study the influence of machining parameters on femtosecond laser drilling of SiC<sub>f</sub>/SiC CMC. The results showed that femtosecond laser does not produce remelting layer, and machining quality has been significantly improved compared with traditional laser machining. However, it may cause taper and spillage, and high laser power easily generates a large splash force which causes damage to micro-holes export. Therefore, the current methods for preparing SiC<sub>f</sub>/SiC CMC micro-holes have limitations.

Ultrasonic vibration-assisted drilling (UVAD) is a new advanced technology that can reduce the cutting force and tool wear, improve the machining quality, and remit the problem of tool fracture to a certain extent. Therefore, it has attracted extensive attention in the field of CMC machining [10–13]. Liu et al. [14] used cemented carbide twist drill to drill two-dimensional orthogonal braided structure carbon fiber reinforced ceramic matrix composites (2D C<sub>f</sub>/SiC CMC). It was noted that CMC is difficult to machine with traditional drills because of terrible tool wear. Feng et al. [15] studied the formation mechanism of tearing defects in rotating ultrasonic machining (RUM) of C<sub>f</sub>/SiC CMC. It was reported that RUM could averagely reduce the tearing defect at the hole exit by more than 60%, which means that the tool wear of RUM is decreased obviously. Wang et al. [16] studied the edge chipping formation mechanism of C<sub>f</sub>/SiC CMC, and the microstructure characteristics of the pore surface under different fiber directions, ultrasonic amplitude, and spindle speed were analyzed. Through theoretical analysis, the fiber fracture mechanism in C<sub>f</sub>/SiC CMC rotating ultrasonic machining is revealed. It was found that the edge chipping size increased with an increase in spindle speed or a decrease in feed rate. While the ultrasonic vibration amplitude only slightly affected the edge chipping size. Tearing defects, edge chipping, and other machining damage can reflect the degree of tool wear to a certain extent, and more machining damage obviously corresponds to more serious tool wear. RUM can reduce machining damage, which means that RUM can significantly reduce tool wear.

Qu et al. [17] investigated the surface grinding mechanisms of 2.5D needle C<sub>f</sub>/SiC CMC. Experiments on the grinding of 2.5D needle C<sub>f</sub>/SiC CMC were performed by a diamond grinding wheel on a surface grinding machine. The experimental results showed that CMC can be machined well with multi-edge tools of grinding wheels. And the machined

surface quality increased with an increase in grinding depth and feed speed and decreased with increasing wheel speed. Yuan et al. [18] applied rotary ultrasonic machining to the surface machining of C<sub>f</sub>/SiC CMC and established the mathematical relationship between cutting parameters and vibration parameters. The cutting force increased with the increase of cutting width and feed rate, whereas the cutting force was found to decrease with the increase of spindle speed. Zhang et al. [19] established the cutting force model of C<sub>f</sub>/SiC CMC based on brittle fracture for rotary ultrasonic surface milling (RUFM) machining, and the established cutting force model is verified by cutting force experiment and simulation. The results showed that the cutting force decreased significantly with the increase of cutting speed, whereas the same was found to increase with the increase of feed rate and cutting depth. It is well known that the greater the cutting force, the more likely the tool is to break. The low cutting force of RUM means that using RUM to machine CMC can significantly reduce the risk of tool breaking.

As can be seen above, the application of ultrasonic vibration can significantly reduce cutting force and machining damage, which means that the tool wear of ultrasonic vibration-assisted machining is obviously decreased. At the same time, ultrasonic vibration-assisted machining can change the contact state between the tool and the workpiece and reduce the friction force and machining temperature. Therefore, it can effectively alleviate the problem of insufficient tool stiffness and wear resistance in micro-hole drilling. However, the current research is focused on the C<sub>f</sub>/SiC CMC and there are few reports on the study of SiC<sub>f</sub>/SiC CMC, which has a higher hardness, brittleness, and stronger bonding strength between fiber and matrix. Besides, the machining of micro-holes with a diameter smaller than 1 mm has not been reported.

In this paper, ultrasonic vibration-assisted drilling is applied for fabricating micro-holes on SiC<sub>f</sub>/SiC CMC. Firstly, the trajectory of single abrasive grains on the tool was established, and the material removal process was analyzed. Then, the comparison experiment of six kinds of cutting tools was carried out. The cutting force, aperture precision of hole, roundness, tear factor, and influence of tool wear regularity of different cutting tools were investigated. Finally, combining theoretical analysis and machining experiments, the most suitable tool for the machining of SiC<sub>f</sub>/SiC CMC micro-holes was found and solved the problem that it is difficult to drill micro-holes (smaller than 1 mm) on SiC<sub>f</sub>/SiC CMC.

## 2 Materials and experimental procedures

### 2.1 Materials

The SiC<sub>f</sub>/SiC CMC consists of three parts: silicon carbide fibers, PyC interface layer (the pyrolysis C interfacial layer



Fig. 1 SiC<sub>f</sub>/SiC CMC

Table 1 Mechanical properties of SiC<sub>f</sub>/SiC CMC

Density	Tensile strength	Bend strength	Compression strength	Fracture toughness
2.26 g/cm <sup>3</sup>	271.4 MPa	443.8 MPa	454 MPa	24.1 MPa·m <sup>1/2</sup>

provides a mechanism for fiber deflection that minimizes crack openings left by matrix cracks.), and silicon carbide matrix. Experiment specimen was produced using the chemical vapor infiltration (CVI) method. The size of SiC<sub>f</sub>/SiC CMC sample is 80 × 45 × 4 mm<sup>3</sup>, and it is shown in Fig. 1. The volume fraction of SiC fiber is about 40%. The thickness of the PyC interphase layer is about 1 μm. The porosity of the composite is about 10%. The mechanical properties at room temperature of the sample are listed in Table 1.

### 2.2 Experimental tools

Six different tools were used in the experiment, as shown in Fig. 2. From left to right, they are carbide drill, PCD drill

(polycrystalline diamond drill), grinding drill (GD), coated grinding drill (CGD), electroplated diamond abrasive tool (EDA), and PDC (polycrystalline diamond compact) drill. Carbide drills and PCD drills are often used to machine plastic materials, while EDA is more commonly used for brittle materials. GD is a kind of drill whose end face is bonded with diamond abrasive grains. Its characteristic is that the cutting edge of the ordinary drill is discrete into several tiny cutting edges, and it has certain self-sharpening. PDC is a tool formed by sintering polycrystalline diamond to a matrix rod under high temperature and pressure (6GPa and 1500 °C). And laser machining is then used to create grooves on the diamond composite for cutting and chip removal, as shown in Fig. 2b.

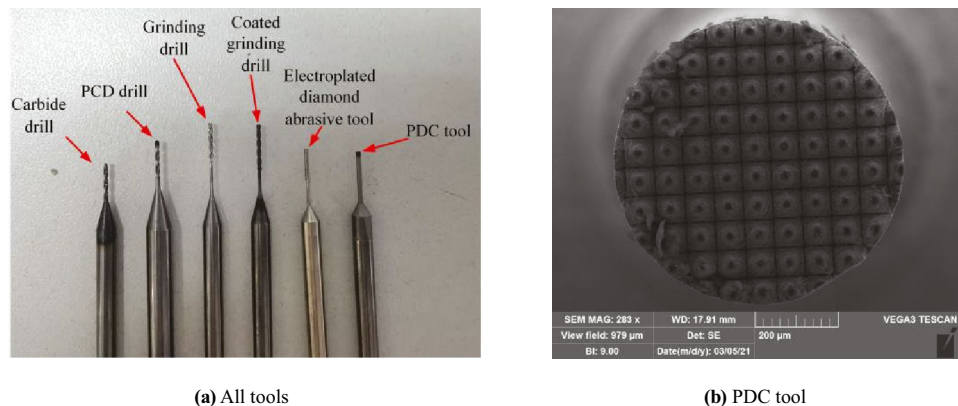
### 2.3 Experimental design and measurement

The tool comparison experiment was carried out on a CY-VMC850 three-axis CNC machine. The ultrasonic tool-holder used was CKN-XH11-BT40, which is supplied by Xi’an Chao Ke Neng Ultrasonic Technology Research Institute Co., Ltd., whose vibration frequency was 30 kHz. The model of ultrasonic power supply is SUM20040771, and the frequency is adjustable from 10 to 50 kHz. Before the experiment, the LK-H020 vibrometer was used to measure and calibrate the amplitude of each tool to ensure that the amplitude of each tool was the same and constant during the machining process. During the test, the cutting force was measured and collected by Kistler 9119AA1 multicomponent dynamometer. The CNC machine, dynamometer, vibrometer, and ultrasonic system are shown in Fig. 3.

The single-factor test method was used to compare the effects of different tools in machining SiC<sub>f</sub>/SiC CMC. The detailed machining parameters are shown in Table 2.

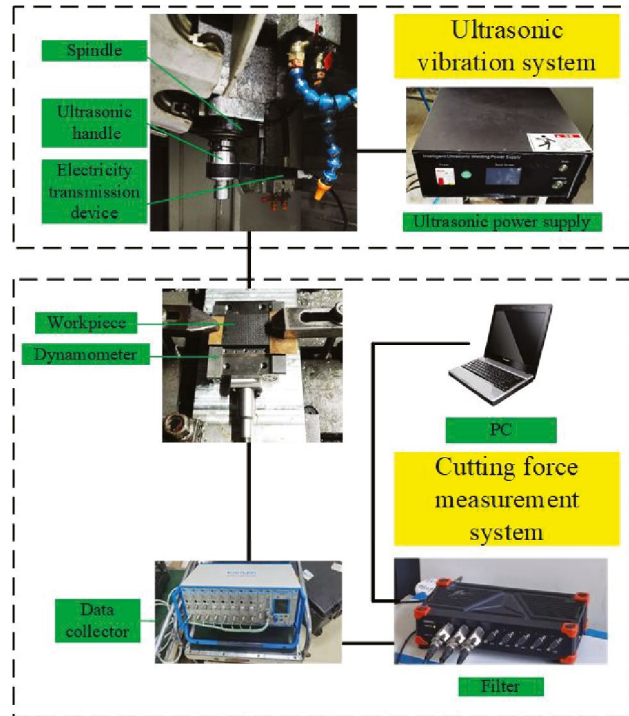
As presented in Fig. 4, after the experiment, VEGA 3 LMU SEM–EDS scanning electron microscope was used to observe the tool wear state, and Alicona IFM-G4 automatic tool scanner was used to measure the hole diameter and roundness.

Fig. 2 The tool used in the experiment. a All tools. b PDC tool





(a) CY-VMC850 three-axis CNC machine



(b) Ultrasonic vibration system and cutting force measurement system

Fig. 3 Experimental equipment. a CY-VMC850 three-axis CNC machine. b Ultrasonic vibration system and cutting force measurement system

Table 2 Experiment parameters

Parameters	Value
Spindle speed/(r/min)	12000
Feed speed/(mm/min)	4
Frequency/kHz	30
Amplitude/ $\mu\text{m}$	4

### 3 Material removal process and discussion

#### 3.1 Grain motion trajectory

Ultrasonic vibration–assisted drilling is a machining method that combines ultrasonic vibration on feed direction with traditional drilling. The cutting tool and the workpiece can

Fig. 4 Experimental measurement equipment. a Automatic tool scanner. b Scanning electron microscope



(a) Automatic tool scanner



(b) Scanning electron microscope

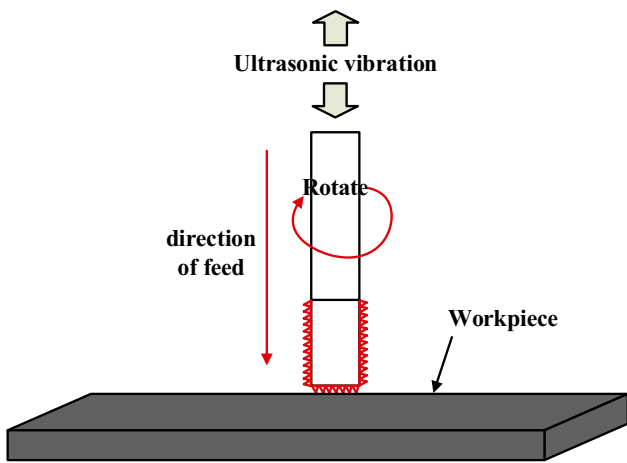


Fig. 5 Diagram of UVAD

contact and separate periodically. In this way, the drilling force, temperature, and tool wear can be reduced [20–22]. Unlike traditional drilling, the movement of the cutting edge (or abrasive grain) on the end face of the tool is a combination of three actions: axial feed, rotation with the spindle, and axial ultrasonic vibration. The schematic diagram of ultrasonic vibration assisted drilling is shown in Fig. 5.

Therefore, the motion trajectory of a single cutting edge (a single abrasive grain) is different from that of conventional drilling (CD). In the CD process, the trajectory of abrasive grains can be expressed as:

$$\begin{cases} x_{CD} = R \cos(\frac{\pi S}{30}t) \\ y_{CD} = R \sin(\frac{\pi S}{30}t) \\ z_{CD} = -vt \end{cases} \quad (1)$$

where  $R$  is the radius of the cutting tool,  $S$  is the spindle speed, and  $t$  is the cutting time. However, due to the introduction of

ultrasonic vibration, the motion trajectory of abrasive grains in the UVAD process changes as follows:

$$\begin{cases} x_{UVAD} = R \cos(\frac{\pi S}{30}t) \\ y_{UVAD} = R \sin(\frac{\pi S}{30}t) \\ z_{UVAD} = -vt + A \sin(2\pi ft + \theta) \end{cases} \quad (2)$$

where  $A$  is the amplitude of ultrasonic vibration,  $f$  is the frequency of ultrasonic vibration, and  $\theta$  is the initial phase angle of ultrasonic vibration. The motion trajectory of a single abrasive grain in UVAD and CD is shown in Fig. 6.

Assuming that the tool has a total of  $n$  abrasive grains on the diameter of abrasive grains, the motion trajectories of different abrasive grains on the tool in CD are as follows:

$$\begin{cases} x_{CDi} = R \cos(\frac{\pi S}{30}t + \frac{2\pi(n_i-1)}{n}) \\ y_{CDi} = R \sin(\frac{\pi S}{30}t + \frac{2\pi(n_i-1)}{n}) \\ z_{CDi} = -vt \end{cases} \quad (3)$$

where  $n_i$  is the serial number of the abrasive grains. Motion trajectories of different abrasive grains on the tool in UVAD are as follows:

$$\begin{cases} x_{UVADi} = R \cos(\frac{\pi S}{30}t + \frac{2\pi(n_i-1)}{n}) \\ y_{UVADi} = R \sin(\frac{\pi S}{30}t + \frac{2\pi(n_i-1)}{n}) \\ z_{UVADi} = -vt + A \sin(2\pi ft + \theta) \end{cases} \quad (4)$$

The motion trajectories of two adjacent abrasive grains in CD and UVAD are shown in Fig. 7. As can be seen from Fig. 7, two adjacent abrasive grains in CD always move in parallel, and their motion trajectories do not interfere with each other. However, in UVAD, the motion trajectories of two adjacent abrasives will cross. In each vibration cycle, the abrasives will only be pressed into the workpiece for a small part of the time so that the cutting temperature is lower, and the cutting depth of each abrasive is

Fig. 6 Comparison of single grain motion trajectories between UVAD and CD

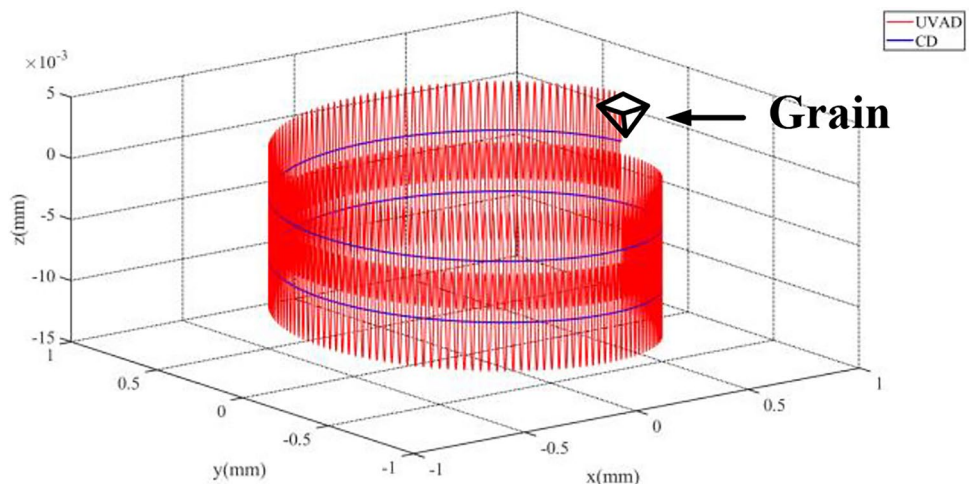
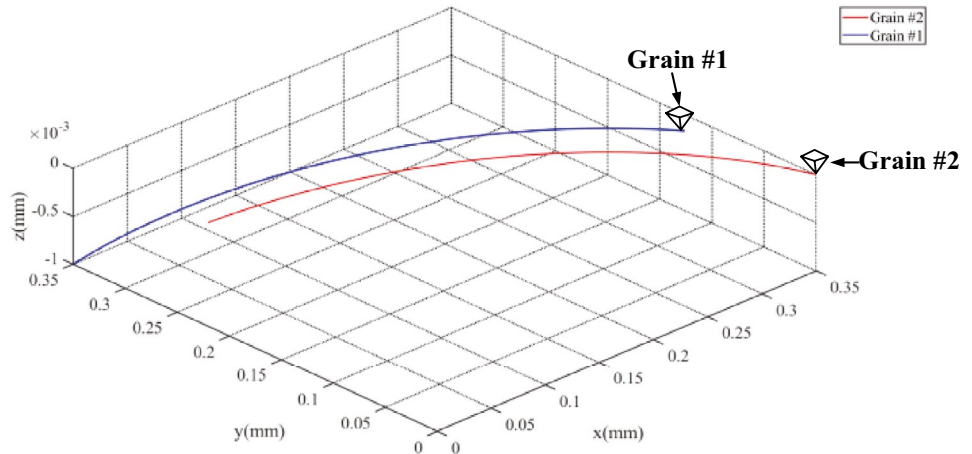
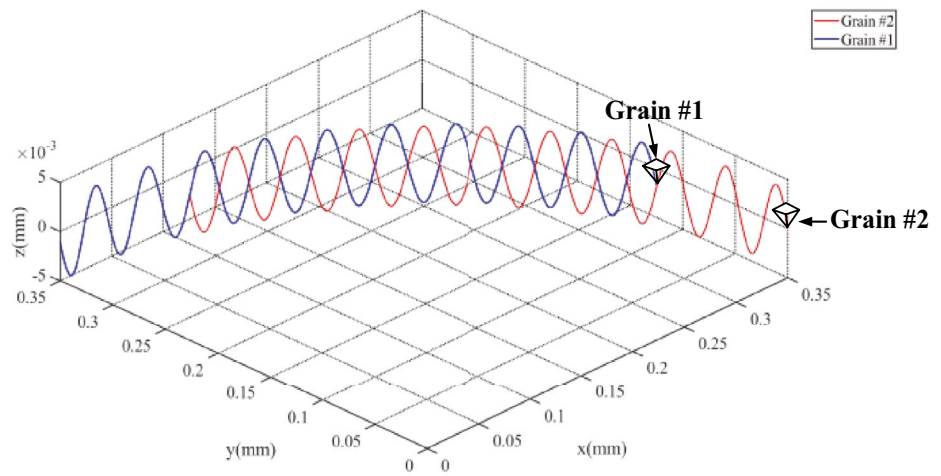


**Fig. 7** Comparison of the motion trajectories of adjacent grains of CD and UVAD. **a** The motion trajectories of two adjacent grains of CD. **b** The motion trajectories of two adjacent grains of UVAD



**(a)** The motion trajectories of two adjacent grains of CD



**(b)** The motion trajectories of two adjacent grains of UVAD

lower than CD most of the time. At the same time, due to the existence of ultrasonic vibration, the abrasive grains are always hammering the workpiece surface, which makes the material easier to be removed and the machining quality is better.

**3.2 Material volume removed by a single abrasive particle in a single vibration period**

Due to the introduction of ultrasonic vibration, the abrasive grains and the surface to be machined are in the discontinuous machining state of “contact-separation-contact,” as shown in Fig. 8. Therefore, the time from zero to the maximum depth of abrasive grains invading the specimen can be described as follows:

$$\begin{cases} t_1 = (1/2\pi f) \arcsin((A - h_m)/A) \\ t_2 = \frac{1}{4f} \end{cases} \quad (5)$$

where  $h_m$  is the maximum depth of abrasive grains invading the workpiece. Therefore, the effective contact time ( $\Delta t$ ):

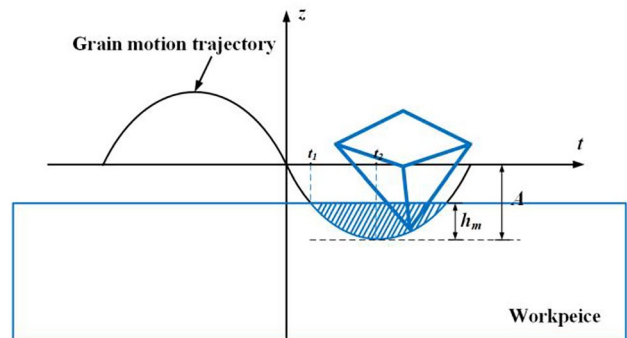


**Fig. 8** Contact diagram of grain and workpiece

$$\Delta t = 2(t_2 - t_1) = \frac{1}{2f} - \left(\frac{1}{\pi f}\right) \arcsin\left(\frac{A-h_m}{A}\right) = (1/\pi f) \arccos((A - h_m)/A) \tag{6}$$

In the effective contact time, the abrasive grains are always rotating with the cutting tool, so the movement distance  $L$  of the abrasive grains with the cutting tool is:

$$L = \frac{2\pi RS t}{60} = \frac{\pi RS \Delta t}{30} \tag{7}$$

According to the fracture mechanics theory, a certain plastic deformation zone will be generated when the tool intrudes into the brittle material. With the increase of the penetration depth of the tool, cracks will be generated in the brittle material. And the crack of brittle material is only related to the volume of the tool intrusion material, independent of the shape of the tool. Therefore, if the size and shape of all diamond abrasives are assumed to be the same and the material is an ideal brittle material with only brittle fracture, the crack size can be calculated by the following equation:

$$\begin{cases} C_L = C_2 \left(\frac{1}{\tan \beta}\right)^{5/12} \left(\frac{E^{3/4}}{H_v K_{IC}(1-\nu^2)^{1/2}}\right)^{1/2} (F_n)^{5/8} \\ C_h = C_2 \left(\frac{1}{\tan \beta}\right)^{1/3} \frac{E^{1/2}}{H_v} (F_n)^{1/2} \end{cases} \tag{8}$$

where  $C_L$  is the lateral crack length,  $C_h$  is the longitudinal crack (median crack) length,  $\beta$  is the apex angle of the abrasive grain,  $\rho$  is the geometric shape parameter of the abrasive grain, and for the four-pyramid type abrasive grain,  $\rho$  is 1.85.  $E$  is the elastic modulus of the material,  $K_{IC}$  is the fracture toughness of the material,  $\nu$  is the Poisson's ratio of the material, and  $H_v$  is the hardness of the material.  $F_n$  is the impact force of a single abrasive grain on the material. According to the research results of Jiao et al. [23],  $F_n$  can be calculated by the following equation:

$$F_n = \frac{1}{2} \rho h^2 \tan^2 \beta H_v \tag{9}$$

Therefore, the crack size can also be expressed as:

$$\begin{cases} C_L = 0.648 C_2 \cdot \rho^{5/8} \cdot \tan^{5/6} \beta \cdot H_v^{1/8} \left(\frac{E^{3/4}}{K_{IC}(1-\nu^2)^{1/2}}\right)^{1/2} \cdot h_m^{5/4} \\ C_h = 0.707 C_2 \cdot (\rho E)^{1/2} \cdot \tan^{2/3} \beta \cdot H_v^{-1/2} \cdot h_m \end{cases} \tag{10}$$

The lateral cracks contact each other or extend to the edge of the material in the expansion process, which will cause the removal of the material. As shown in Fig. 9, Longitudinal crack (median crack) is the main cause of subsurface crack of the machined surface. Therefore, within the effective contact time of a single vibration period, the material volume removed by a single abrasive grain is:

$$V_R = 2V_{ABCD} = \frac{1}{3} C_L C_h L \tag{11}$$

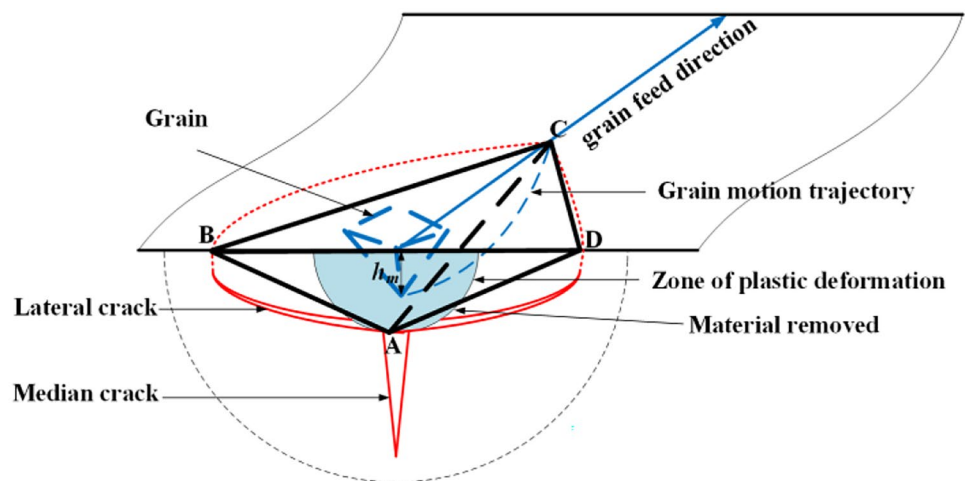
Substituting Eqs. (6), (7), and (10) into Eq. (11), we can get:

$$V_R = 0.0078 \rho^{9/8} \cdot \tan^{3/2} \beta \cdot H_v^{-3/8} \left(\frac{E^7}{K_{IC}(1-\nu^2)^{1/2}}\right)^{1/2} \cdot h_m^{9/4} \frac{RS}{30f} \arccos\left(\frac{A-h_m}{A}\right) \tag{12}$$

### 3.3 Discussion

According to Eq. (12), the volume of material removed by a single abrasive (single tool edge) in a single vibration period ( $V_R$ ) is related to not only material properties, machining parameters and ultrasonic parameters but also geometric parameters  $\rho$ , apex angle  $\beta$  of the abrasive or blade on the tool and depth of abrasive penetration into the material ( $h_m$ ).

Fig. 9 Material removal process diagram



However, in the actual machining process, in addition to the above factors, the machining performance of the tool is also related to the number of abrasive grains on the tool. This is because the amount of material to be removed is fixed in machining. When the number of abrasive grains is low, the total volume of material removed by a single abrasive grain goes up, and the cumulative penetration depth of material invaded by a single abrasive grain needs to be increased. This obviously leads to increased tool wear and even tool failure.

Traditional drilling tools such as carbide drills and PCD drills have only two blades, the tool in addition to the axial invasion of material, but also with the rotation of the tool in the circumferential invasion of material constantly to remove material in drilling machining. In this process, in addition to the drill tip, the blade also keeps rubbing against a hard material, which results in severe tool wear. Combined with the large amount of volume that a single blade needs to remove, the increase in the cumulative penetration depth of material invaded by a single abrasive grain can lead to increased tool wear. Therefore, there may be too serious wear problem when using traditional carbide drills and PCD drills to drill SiC<sub>f</sub>/SiC CMC material in actual machining.

When using GD and CGD to process SiC<sub>f</sub>/SiC CMC, it is not the blade of the drill that is machined but the abrasive grains on the blade. The abrasive grains on the blade are irregular in shape; most of them are five-pyramid, which have large  $\rho$ . Therefore, the  $V_R$  is large, which means that the volume of chips produced is large. Therefore, the machining accuracy will be insufficient. However, the size of the abrasive grain is very small (250#), the gap between the abrasive grains is very small, and the large volume chip is easy to plug the gap between the abrasive grains, resulting in tool passivation and machining performance decline, which result in machining accuracy is further reduced. Therefore, the use of GD and CGD may lead to low machining accuracy when machining SiC<sub>f</sub>/SiC CMC.

The machining situation of EDA is similar to GD and CGD, but the difference lies in that the EDA does not have a chip groove. The abrasive size of the EDA is 200#, and the abrasive size is larger than GD and CGD. The number of abrasive grains on the end face of EDA is also much larger than GD and CGD. Since there is no chip groove, the chip will stay on the contact surface of the tool and the workpiece. Consequently, it keeps rubbing the abrasive grains, leading to excessive tool wear. Therefore, EDAs euhedral lower tool life than GD and CGD. However, due to a large number of abrasive grains on the end face of EDA, the total volume of abrasive grains removed by a single grinding head is lower than that of GD and CGD. The tool passivation will be reduced due to the larger abrasive size and the larger abrasive gap. Due to these two reasons, the EDA will show better machining accuracy than the two kinds of grinding heads.

Therefore, the use of EDA may lead to higher machining accuracy but lower tool life when machining SiC<sub>f</sub>/SiC CMC.

PDC tools are machined using polycrystalline diamond cutting blocks (which can be regarded as diamond abrasive grains) on the end face when machining SiC<sub>f</sub>/SiC CMC. The diamond cutting blocks on the end face are regular four-pyramid shapes with low  $\rho$ . So, the  $V_R$  is small, that is, the volume of chip generation is small, and the machining accuracy is high. At the same time, because the diamond cutting blocks and the tool are in one piece, so the control strength is high. Diamond cutting blocks do not fall off in most cases, although they are wearing to a certain extent. The actual number of abrasive grains involved in the machining is the total amount of end face cutting blocks. Therefore, when PDC tools processed SiC, the total amount of material removed by single abrasive grain is minimum, and the machining accuracy is high. The cutting block of the PDC cutter is machined, and its apex angle  $\beta$  can be controlled. The  $\beta$  can be made smaller when making the tool so that  $V_R$  can be further reduced, thus improving the machining accuracy. In addition, the length, width, and height of diamond cutting blocks are 0.07 mm, and the gap between the cutting blocks is large. So, the wear between the chip and abrasive grains is significantly alleviated compared with the EDA. Therefore, the use of EDA may lead to higher machining accuracy and higher tool life when machining SiC<sub>f</sub>/SiC CMC.

In summary, according to Eq. (12) and theoretical analysis, PDC tools are the most suitable tool for SiC<sub>f</sub>/SiC CMC drilling.

### 3.4 Drilling force

According to the results of the experimental tests shown in Table 3, it could be found that PCD drill and carbide drill cannot be used to drill the sample. In accordance with the above conclusions, it is difficult to drill SiC<sub>f</sub>/SiC CMC samples with single or double edge tools such as traditional drill drills. The GD, CGD, EDA, and PDC tools were all successfully drilled on the sample. However, the distribution of abrasive grains on the GD has great randomness, and the coating amplifies its inhomogeneity. This causes

**Table 3** Experiment results

Tool type	Machining results
Carbide drill	Tool break
PCD drill	Tool break
GD	Drilling success
CGD	Some drills successfully drilled holes (with a great randomness)
EDA	Drilling success
PDC tool	Drilling success



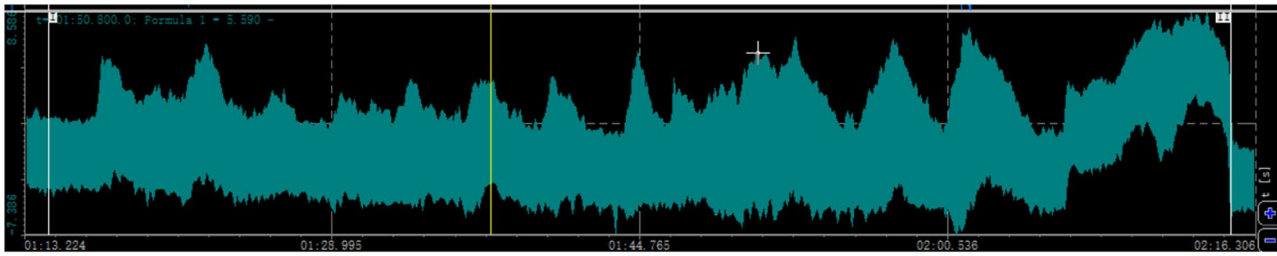


**Fig. 10** Instantaneous drilling force of EDA

the machining results of the CGD having great randomness. Some of the tools are very easy to break, while the others' machining effect is excellent.

The cutting force is an important parameter for tool selection as it could reflect the tool wear and machining quality. Figure 10 shows the cutting force signal of the GD. The cutting force signals show an obvious fiber layer correlation. Also, the cutting force changes with different cutting layers. Meanwhile, the number of changes is consistent with the number of fiber layers. The peak value of cutting force appears at the end of the hole making process, which is the exit of the hole. The time of cutting force signal in this layer is prolonged. The reason is that the material thickness that supports the axial cutting force at the exit of the hole is thin, and it is easy to bend because of the axial cutting force. Therefore, the machining time at the exit of the hole is prolonged. At the same time, the bending of the material provides an additional elastic force to the tool, resulting in an increase in cutting force.

The cutting force data of different tools are shown in Fig. 11. For the average cutting force, GD is the largest, followed by CGD. PDC is slightly larger than EDA but significantly lower than GD and CGD; for peak cutting forces,

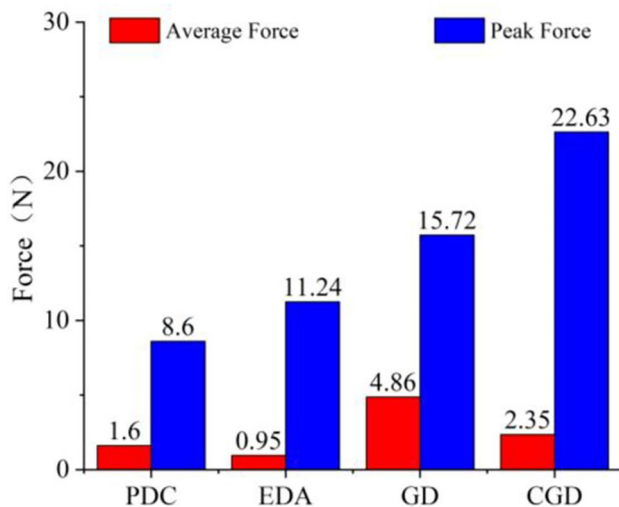


**Fig. 11** Comparison of drilling forces of different tools

CGD is the largest. Although the peak cutting force of EDA is lower than GD, it is still significantly higher than PDC. As the diameter of the tool is 0.7 mm, the rigidity of the tool is seriously insufficient. Therefore, the peak cutting force can reflect the possibility of tool fracture to some extent. Thus, the GD and CGD may be broken during machining. At the same time, due to the additional peak force when the coating of the CGD ruptures, the machining performance of the CGD is accompanied by a great randomness. Therefore, both in terms of average and peak cutting forces, EDA and PDC tools are more suitable for machining  $\text{SiC}_f/\text{SiC}$  CMC.

### 3.5 Machining accuracy

For gas film holes, hole machining accuracy such as hole diameter and roundness will not only change the gas flow of the hole and thus affect the quality of the gas film but also affect the life of components. Therefore, the accuracy of hole machining is another important factor that should be considered for choosing cutting tools. Figures 12, 13, 14, and 15 present the micro-holes drilled by different tools during ultrasonic vibration assisted drilling  $\text{SiC}_f/\text{SiC}$  CMC, and the hole morphology of entrance and outlet was investigated using a scanning electron microscope.

The hole diameter, taper, and roundness of its entrance and outlet are shown in Figs. 16 and 17. It can be seen that the test results are consistent with the analysis in Sect. 3.1. The holes machined with PDC tools have the best hole diameter and roundness, followed by EDA. The holes machined with GD and CGD have the worst machining accuracy. This is because when using EDA, GD, and CGD, there are problems with large  $V_R$  and small abrasive grains gap, resulting in the reduction of machining accuracy. At the same time, due to the small number of abrasive grains on the end face of GD and CGD, the total volume of material removed by a single abrasive grain is larger, which further reduces the machining accuracy. PDC tool  $V_R$  is relatively small; the volume of chip generation is also small. At the same time, the distance between cutting edges is larger, more chips can be accommodated, and the degree of tool passivation is lower.

**Fig. 12** Hole morphology of GD. **a** The entrance hole. **b** The outlet hole

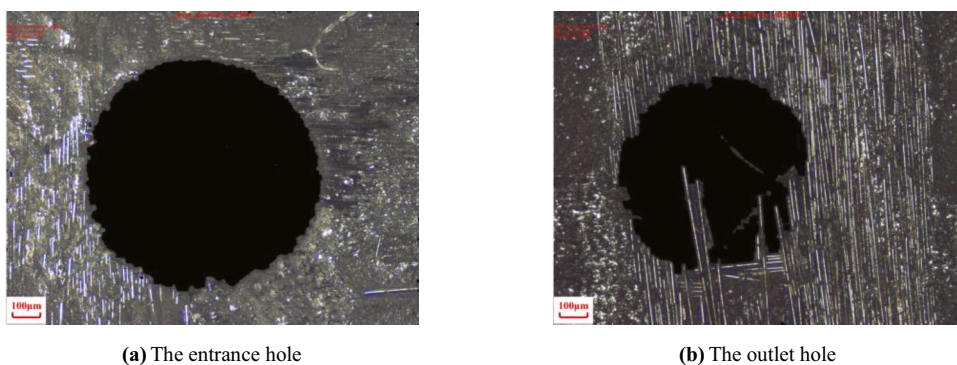


**Fig. 13** Hole morphology of CGD. **a** The entrance hole. **b** The outlet hole

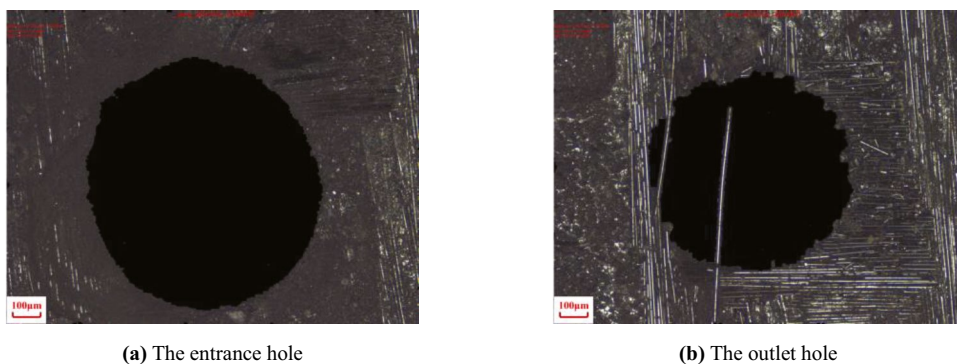
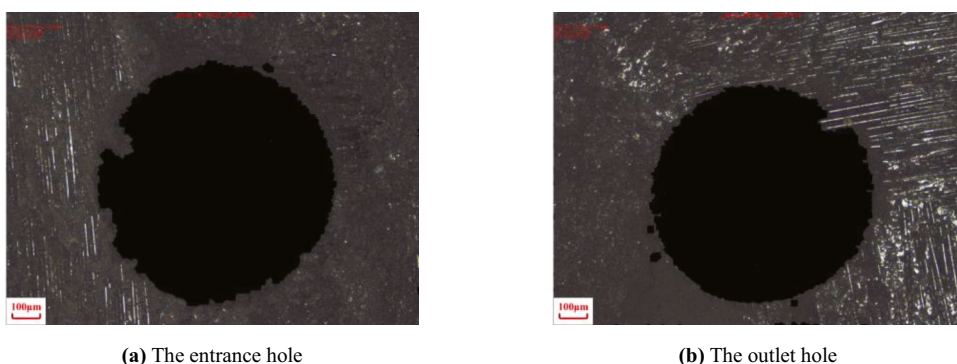


**Fig. 14** Hole morphology of EDA. **a** The entrance hole. **b** The outlet hole



And all the PDC tool is diamond, even if the cutting edge is wear, it still has good machining ability.

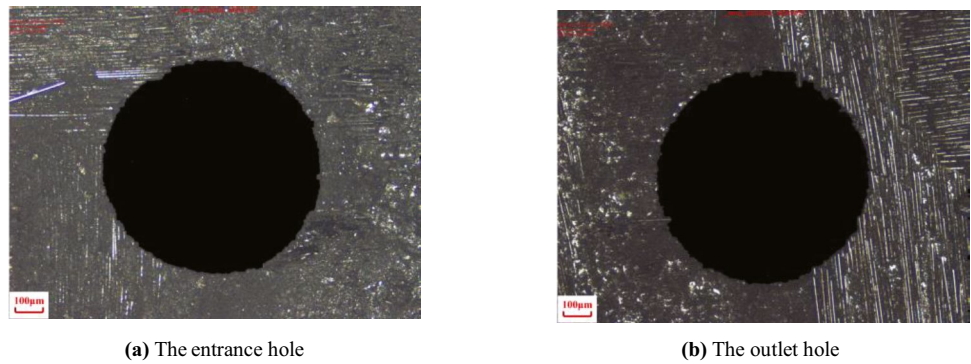
Therefore, in terms of machining accuracy such as hole diameter, taper, and roundness, the PDC tool shows better machining performance than the other three tools. For the parts that require high machining accuracy of hole machining, the PDC tool should be preferred.

### 3.6 Tool wear

As the tool diameter is very small, the rigidity of the tool is not very high. Therefore, the primary consideration for the machining of 0.7-mm micro-holes is the tool life. The tool wear is an important factor to reflect the tool life and

machining performance. Figures 18, 19, 20, and 21 are the comparison diagram of the tool appearance of four kinds of tools before and after machining, which can clearly reflect the tool wear. In Fig. 18, the EDA has the most severe wear. After machining, the abrasive grains on the tool face are all off, and the tool no longer has machining performance. This is because the abrasive grains of the electroplated diamond grinding head are only bonded together with the substrate or rod of the coating through mechanical inlaying, and the bonding strength is low. At the same time, because the machining is not allowed to add coolant, the accumulated heat of machining cannot be emitted. The accumulated heat may result in the softening of the coating substrate, and the holding strength of the abrasive grains is further reduced.

**Fig. 15** Hole morphology of PDC tool. **a** The entrance hole. **b** The outlet hole



As we can see in Figs. 18, 19, 20, and 21, for the tool wear, PDC, and CGD have minor tool wear, while GD has slightly more severe tool wear. But the tool wear of EDA is very serious. However, the wear of GD and CGD is similar, mainly manifested as the breakdown and shedding of abrasive grains, as shown in Figs. 19 and 20. In Fig. 20, after machining, the coating of the CGD is completely removed and the coating is no longer visible on the end face. This is because the coating and the surface to be processed are surface contact state. The coating is brittle, and it is easy to be broken in the process and causes a large area of fall off. This is also one of the reasons why the peak cutting force of CGD is greater than that of the PDC tool. Although the cutting force of the CGD is very small before the coating is

removed, the machining state of the CGD after the coating is removed is the same as that of the GD. The peeling of the coating can also easily lead to the enhancement of tool instability, which is the reason for the instability of the machining performance of the CGD.

The cutting-edge wear of the PDC tool is mainly concentrated in the center of the tool. This is because the closer to the center of the tool, the lower the linear velocity of the cutting edge, so the more serious the wear will be. At the same time, the chip generated by machining will be more stacked in the position of the tool center, the friction between the micro cutting edge and the chip in the center position is more serious, so the micro cutting edge in the center position wears faster. PDC tool is a tool formed by sintering polycrystalline diamond micro powder to a matrix rod under high temperature and pressure. So, after the diamond cutting blocks is blunt, it still has a considerable machining performance because of the polycrystalline diamond micro powder.

Meanwhile, the PDC tool's diamond cutting blocks after the blunt, can also be laser machined at a relatively low price. Although all four tools have some degree of wear, PDC tools are still the most suitable tool for machining SiC<sub>f</sub>/SiC CMC.

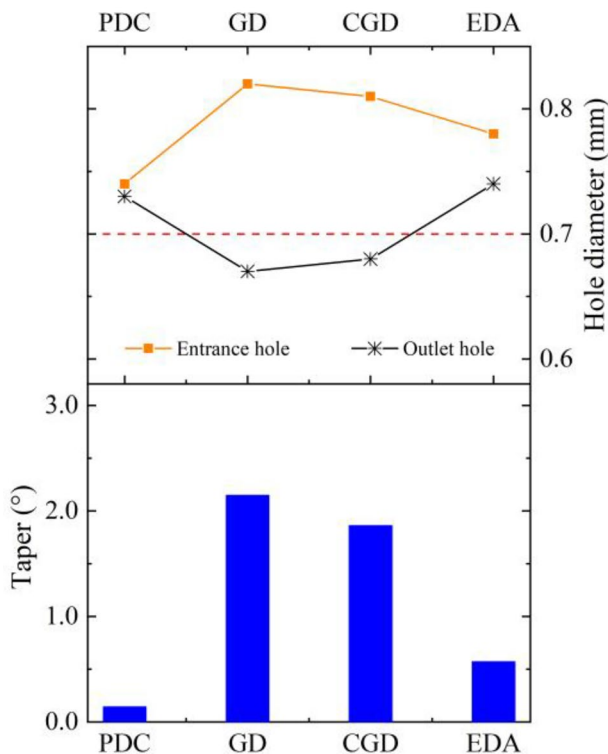


**Fig. 16** Comparison of hole diameter and taper of different tool types

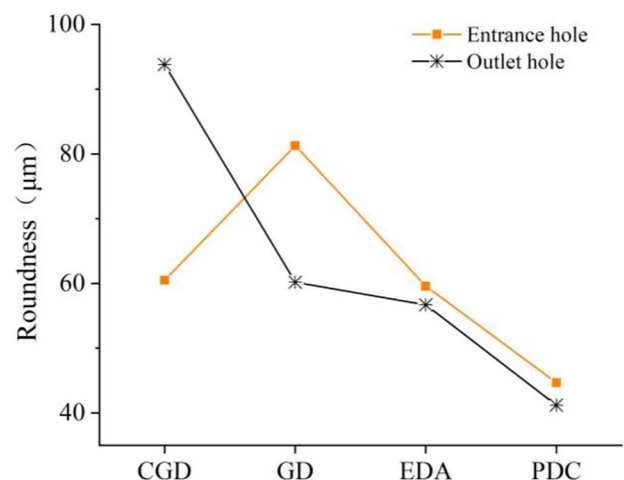
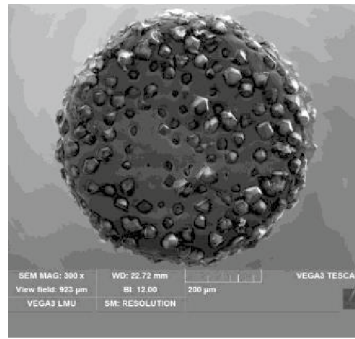
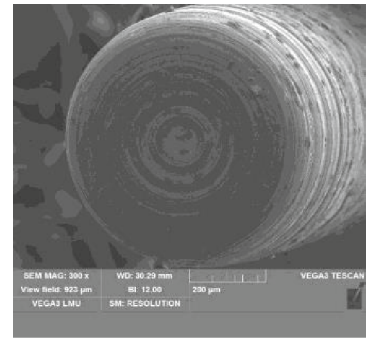


**Fig. 17** Comparison of roundness of different cutting tools

**Fig. 18** Wear condition of EDA. **a** New tool. **b** Worn tool

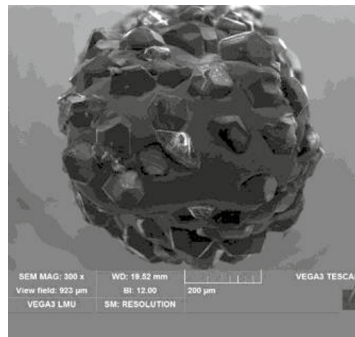


**(a)** New tool

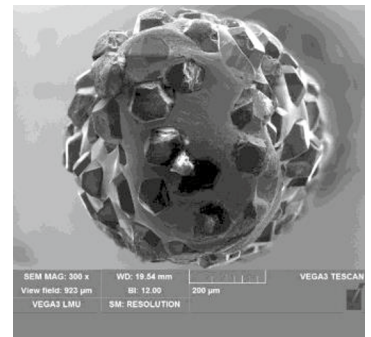


**(b)** Worn tool

**Fig. 19** Wear condition of GD. **a** New tool. **b** Worn tool

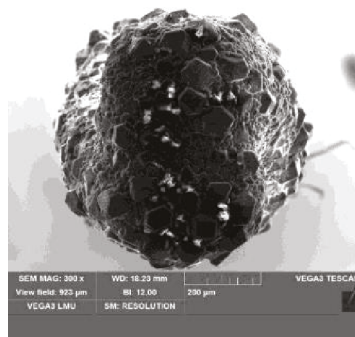


**(a)** New tool



**(b)** Worn tool

**Fig. 20** Wear condition of CGD. **a** New tool. **b** Worn tool

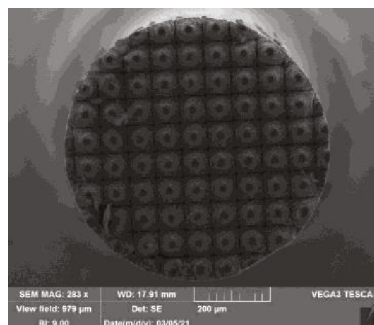


**(a)** New tool

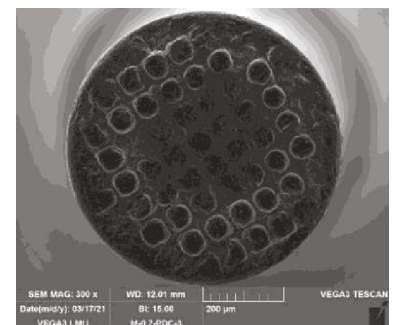


**(b)** Worn tool

**Fig. 21** Wear condition of PDC tool. **a** New tool. **b** Worn tool



**(a)** New tool



**(b)** Worn tool

## 4 Conclusions

Based on the theoretical and experimental analysis, the material removal process of SiC<sub>f</sub>/SiC CMC was investigated and the effects of different kinds of tools on cutting force, machining accuracy, and tool wear during ultrasonic vibration assisted drilling of SiC<sub>f</sub>/SiC CMC were revealed. From the experimental results and analysis, the following conclusions can be drawn:

- (1) The material removal process under the action of the ultrasonic energy field was analyzed. The results showed that PDC tools are more suitable for machining SiC<sub>f</sub>/SiC CMC. The result of theoretical analysis is verified by experiments.
- (2) In terms of both average and peak forces, the drilling force of the PDC tool and coated grinding drill is significantly smaller than the electroplated diamond abrasive tool and grinding drill. The machining accuracy showed a positive correlation with the drilling force. In this work, the machining accuracy of the PDC tool is best, followed by the electroplated diamond abrasive tool. The machining accuracy of the grinding drill and coated grinding drill is poor with little difference.
- (3) The results of tool wear are in agreement with those of theoretical analysis. PDC and coated grinding drill has minor tool wear while grinding drill has a slightly more severe tool wear. But the tool wear of electroplated diamond abrasive tool is very serious. Therefore, in terms of machining quality and tool life, PDC tools are more suitable for machining SiC<sub>f</sub>/SiC CMC.

In order to deeply understand the ultrasonic vibration-assisted hole making of SiC<sub>f</sub>/SiC CMC, more research should be carried out in the future on the aspects of the cutting force model, material removal mechanism, and machining damage formation mechanism.

**Acknowledgements** Many thanks to the ultrasonic vibration equipment supported by Xi'an Chao Ke Neng Ultrasonic Technology Research Institute Co., Ltd.

**Author contribution** Bo Huang: The guidance and planning of the overall thinking, optimized and guided the experimental process, performed data measurement and analysis, wrote the first draft and revised the contents of the first draft. Wenhui Wang: Provided financial support for materials and equipment, supervision, and reviewing the first draft. Ruisong Jiang: Checking and reviewing the first draft. Yifeng Xiong: Responsible for the planning of the overall thinking, experimental process, and data analysis, revised and reviewed the first draft. Cong Liu: Assisted in conducting experiments and revising the draft.

**Funding** This work is sponsored by the Special Fund Project for Independent Technology Innovation of Aero Engine Corporation of China (Grant No. ZZCX-2019-022) and China Postdoctoral Science Foundation (Grant No. 2020M683569).

**Data availability** All authors confirm that the data supporting the findings of this study are available within the article.

**Code availability** Not applicable.

## Declarations

**Ethics approval** The manuscript has not been submitted to any other journal for simultaneous consideration. The submitted work is original and has not been published elsewhere in any form or language.

**Consent to participate** All authors voluntarily agree to participate in this research study.

**Consent for publication** All authors voluntarily agree to publish in this research study.

**Conflict of interest** The authors declare no competing interests.

## References

1. Yu H, Fitriani P, Lee S (2015) Fabrication of the tube-shaped SiC<sub>f</sub>/SiC by hot pressing. *Ceram Int* 41(6):7890–7896
2. Kollins K, Przybyla C, Amer M (2018) Residual stress measurements in melt infiltrated SiC/SiC ceramic matrix composites using Raman spectroscopy. *J Eur Ceram Soc* 38(7):2784–2791
3. Liu X, Shen X, Gong L (2018) Multi-scale thermodynamic analysis method for 2D SiC/SiC composite turbine guide vanes. *Chinese J Aeronaut* 31(1):117–125
4. Hui X, Xu Y, Hou Y (2020) A coupled micro-meso-scale study on the damage mechanism of 2D SiC/SiC ceramic matrix composites. *Mech Adv Mater Struc* 28(20):2083–2095
5. Bao Y, Bi M, Gao H (2013) Effect of Fiber Directions on the Surface Quality of Milling C/SiC Composites. *Adv Mat Res* 797:196–201
6. Diaz O, Axinte D (2018) Novovic D. Probabilistic modelling of tool unbalance during cutting of hard-heterogeneous materials: A case study in Ceramic matrix composites (CMCs). *Compos B Eng* 148:217–226
7. Jiao J, Wang Y, Qiu H (2014) Morphology analysis of SiC<sub>f</sub>/SiC Ceramic Matrix Composites machining surface with different machining technology. *Aeronaut Manuf Technol* 06:89–92
8. Kliuev M (2019) EDM Drilling and Milling of Aerospace Materials. ETH Zürich, Switzerland (Doctoral dissertation)
9. Wang C, Zhang L, Liu Y (2013) Ultra-short pulse laser deep drilling of C/SiC composites in air. *Appl Phys A Mater* 111(4):1213–1219
10. Tawakoli T, Azarhoushang B (2011) Intermittent grinding of ceramic matrix composites (CMCs) utilizing a developed segmented wheel. *Int J Mach Tools Manuf* 51(2):112–119
11. Liu J, Zhang D, Qin L (2012) Feasibility study of the rotary ultrasonic elliptical machining of carbon fiber reinforced plastics (CFRP). *Int J Mach Tools Manuf* 53(1):141–150
12. Wang Y, Lin B, Wang S (2014) Study on the system matching of ultrasonic vibration assisted grinding for hard and brittle materials machining. *Int J Mach Tools Manuf* 77:66–73
13. Ning F, Cong W, Pei Z (2016) Rotary ultrasonic machining of CFRP: A comparison with grinding. *Ultrasonics* 66:125–132
14. Liu J, Li H, Zhang X (2012) Investigation of grinding characteristics and removal mechanisms of 2D-C/SiC in high speed deep grinding. *Acta Mater Compos Sin* 29(4):113–118
15. Feng P, Wang J, Zhang J (2017) Drilling induced tearing defects in rotary ultrasonic machining of C/SiC composites. *Ceram Int* 43(1):791–799

16. Wang J, Feng P, Zhang J (2016) Modeling the dependency of edge chipping size on the material properties and cutting force for rotary ultrasonic drilling of brittle materials. *Int J Mach Tools Manuf* 101:18–27
17. Qu S, Gong Y, Yang Y (2018) Surface topography and roughness of silicon carbide ceramic matrix composites. *Ceram Int* 44(12):14742–14753
18. Yuan S, Fan H, Amin M (2016) A cutting force prediction dynamic model for side milling of ceramic matrix composites C/SiC based on rotary ultrasonic machining. *Int J Adv Manuf Tech* 86(1–4):37–48
19. Zhang C, Yuan S, Amin M (2016) Development of a cutting force prediction model based on brittle fracture for C/SiC in rotary ultrasonic facing milling. *Int J Adv Manuf Tech* 85(1–4):573–583
20. Geng D, Zhang D, Xu Y, Jiang X (2015) Effect of speed ratio in edge routing of carbon fiber-reinforced plastics by rotary ultrasonic elliptical machining. *J Reinf Plast Compos* 32(21):1779–1790
21. Bertsche E, Bertsche E, Ehmann K (2013) An analytical model of rotary ultrasonic milling. *Int J Adv Manuf Tech* 65(9):1705–1720
22. Diaz O, Axinte D, Butler-Smith P (2019) On understanding the microstructure of SiC/SiC Ceramic matrix composites (CMCs) after a material removal process. *Ma Sci Eng A Struct* 743:1–11
23. Jiao F, Zhao B, Liu C (2008) Material Removal Rate Characteristics in Ultrasonic Aided Lapping of Engineering Ceramics Based on Single-Point Scratch. *Key Eng Mater* 375–376:263–267

**Publisher's Note** Springer Nature remains neutral with regard to jurisdictional claims in published maps and institutional affiliations.